

# Investigation on a scroll expander for waste heat recovery on internal combustion engines

A. Legros<sup>1, 2</sup>, L. Guillaume<sup>2</sup>, V. Lemort<sup>2</sup>, M. Diny<sup>1</sup>, I. Bell<sup>2</sup> and S. Quoilin<sup>2</sup>

<sup>1</sup>DRD/DRIA/APWE, PSA Peugeot Citroen, France

<sup>2</sup>Thermodynamics Laboratory, University of Liège, Belgium

## ABSTRACT

In the present article, a model of scroll expander will be introduced. This model is able to evaluate the performance of a given machine with influence of the geometry. Several losses are also included by the model such as internal leakages, heat transfers or mechanical losses. The forces generated by the gas pressure on the involutes can also be calculated.

That expander model is used in order to demonstrate its potential and provide some guidelines to the design of a new expander suitable for the application.

## 0. NOTATIONS

### 0.1 Mathematical symbols

$A$	Area	$m^2$	$Pr$	Prandtl number	–
$D_h$	Hydraulic diameter	$m$	$\dot{Q}$	Heat transfer rate	$W$
$f$	Friction coefficient	–	$Re$	Reynolds number	–
$h$	Specific enthalpy	$J/kg$	$r_b$	Base radius	$m$
$H$	Height	$m$	$r_v$	Volume ratio	–
$K_1, K_2$	Coefficients	–	$t$	Wall thickness	$m$
$L$	Length	$m$	$U$	Internal energy	$J$
$\dot{M}$	Mass flow rate	$kg/s$	$V$	Volume	$m^3$
$n$	Normal direction	$m$	$x, y$	x and y coordinates	$m$
$P$	Pressure	$Pa$	$\dot{W}$	Power	$W$

### 0.2 Greek letters

$\gamma$	Heat capacity ratio	–	$\rho$	Density	$kg/m^3$
$\epsilon$	Efficiency	–	$\varphi$	Construction angle	$rad$
$\Delta P$	Pressure difference	$Pa$	$\varphi_0$	Initial angle	$rad$
$\theta$	Crank angle	$rad$	$\omega$	Angular velocity	$rad/s$
$\lambda$	Thermal conductivity	$W/(m K)$			

### 0.3 Subscripts

$ax$	Axial		$o$	Outer involute
$h$	High pressure side		$out$	Coming out of the chamber
$i$	Inner involute		$s$	Isentropic
$in$	Coming in the chamber		$rad$	Radial
$l$	Low pressure side		$x, y$	According to the x or y axis
$loss$	Losses			

## 1. INTRODUCTION

Waste heat recovery Rankine cycle on mobile application is not a new idea. A first concept on a train has already been commercialized in the 1920s, taking advantage of the price difference between diesel and coal [1]. Unfortunately, this system quickly became not competitive because that difference was not profitable anymore. The research on WHR systems rose when oil crisis occurred, in the 1970s. Several systems were developed, mostly for trucks or marine applications. After that period, the interest disappeared until the 2000s, when automotive manufacturers started being interested in that technology again. Actually, due to the restrictive standards on CO<sub>2</sub> emissions placed by Europe, it is necessary to find new ways to reduce car consumption and, thus, improve overall engine efficiency. Waste heat recovery technologies are among the possible solutions. This work focuses on Rankine cycles, mainly because of its potential in efficiency and produced power, demonstrated in previous simulation works [2, 3].

The present article studies a waste heat recovery Rankine cycle for conventional gasoline engines. The first part will present a model of a scroll expander developed to evaluate the performances of a scroll expander considering various parameters such as geometry, internal leakages, heat transfers or mechanical losses. The second part will present some simulation results and provide some guidelines to the design of an expander.

The experimental investigations are currently conducted and the results of the calibration will be written soon.

## 2. MODELIZATION OF THE SCROLL EXPANDER

Several complex models for scroll compressors have already been developed and are available in literature [4, 5] whereas only one work has been for scroll expanders [6]. The work presented in this paper is based mainly on those three thesis. The goal of this model is to be able to size an expander and design one that is adapted to waste heat recovery in a light vehicle.

The model presented here is split into two consecutive sub-models. The first one describes the geometry based on several input parameters and evaluates different geometrical characteristics. The last one is about the thermodynamic evolution of the fluid inside the machine and is able to provide the fluid state in each chamber at every moment of a revolution. This sub-model also evaluates the performances of the machine, the efficiencies and the produced work by calculating the frictional losses and other kinds of losses. Lastly, an additional part of that sub-model consists in evaluating the resultant forces on the moving involutes. Those forces can be used in order to size the shaft and the bearings for example.

The scroll model has been developed in Matlab and the thermodynamic properties are evaluated with Refprop library. A huge effort has been placed on the numerical side. In order to decrease the computation time, lookup tables are generated before the first simulation and interpolations are used inside those tables to evaluate the properties. This can decrease the computation time up to 20%. Additional work has been carried out to decrease the CPU time but it's not presented here.

### 2.1 Geometric sub-model

The profile of a scroll spiral is usually a circle involute. The Cartesian equation system for the circle involute is given by:

$$\begin{cases} x = r_b(\cos(\varphi) + (\varphi - \varphi_0) \sin(\varphi)) \\ y = r_b(\sin(\varphi) - (\varphi - \varphi_0) \cos(\varphi)) \end{cases}$$

Each spiral consists of two circle involutes whose only initial angles  $\varphi_0$  are different and those two curves are named inner and outer involutes. Those two involutes produce a spiral whose thickness is constant and equal to

$$t = r_b(\varphi_{i,0} - \varphi_{o,0})$$

In scroll compressors, the central tip geometry is not a circle involute because this would lead to design that would be difficult to machine. The linking curves between the inner and outer involutes could consist of two circle arcs [7]. Those arcs are tangent to each other and to its neighboring involute. Those conditions provide an equations system with infinity of solutions. One parameter can be set in order to adjust the design and needs to be imposed for the uniqueness of the solution.

Once the geometry is defined, the geometry sub-model evaluates the geometric characteristics over one revolution that will be useful to the other sub-model, such as chamber volumes, heat transfer areas, leakage areas, etc.

Almost every characteristic is based on the determination of the limits of each chamber. The limits are defined by the "contact" points between the two spirals. Those points are called conjugacy points and can be represented by a conjugacy angle, written  $\varphi_{conj}$  with i- or o- subscript depending on which involute is considered (inner or outer). Based on those angles every other geometric characteristic is numerically evaluated by special algorithms. Note that most of the characteristics can also be derived from analytical expressions but the peculiar tip geometry requires some numerical tools because analytical expressions do not exist.

The interference between the moving spiral and the supply port can be evaluated using a specific Matlab function. However those functions are time consumers and it is indeed better to avoid using them. In order to decrease the calculation time, a detection algorithm has been implemented in order to guess when the interference will happen and then start using the interference Matlab functions.

The volume of the different chambers are present in Figure 1. In this Figure, it can be seen the evolution of the different volumes of each pocket of fluid. The clearance volume is displayed and it corresponds to the minimal volume of the suction chamber. A saturation lower limit has been imposed of the discharge volume in order to avoid too small crank angle step.

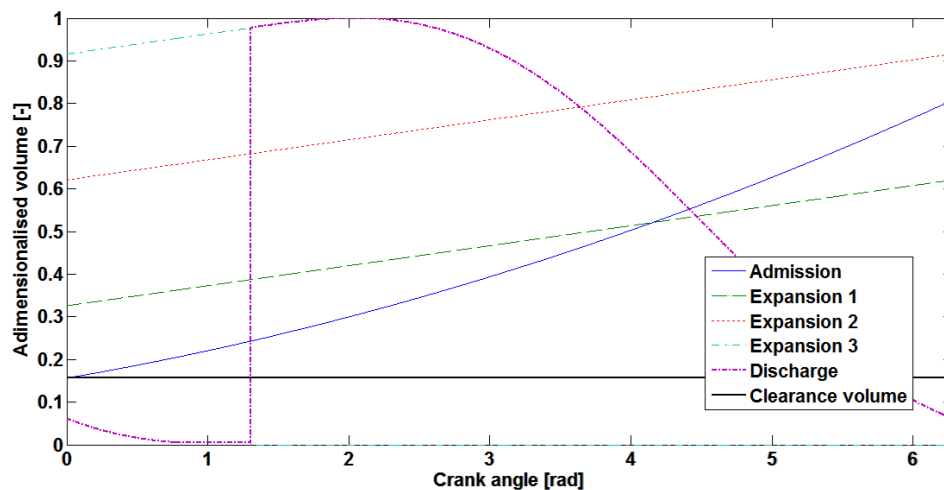


Figure 1 : Adimensionalised volume – given by the division of the actual volume by a constant one - of the different chambers. The clearance volume is also displayed.

## 2.2 Thermo-mechanical sub-model

### 2.2.1 Global considerations

This sub-model is an iterative model on the exhaust enthalpy. The exhaust enthalpy is evaluated after every complete revolution of the scroll expander. Then a convergence criteria based on that enthalpy is checked and the algorithm decides whether or not another revolution is necessary.

One revolution is divided in several constant crank angle steps. The algorithm is sub divided in three parts which are consecutively run at every step of the complete revolution. Those calculations are done simultaneously in every chamber of the expander in order to reduce the calculation time. The three parts are the update of the thermodynamic variables, the evaluation of the different mass flows and the calculations of the heat transfers. They will be described in the next sub-sections.

### 2.2.2 Thermodynamic variables

In the first part, every useful thermodynamic variable, i.e. pressure, temperature, enthalpy, entropy, specific volume and quality, are evaluated based on the determination of the internal energy and the mass of fluid in the chambers. In order to evaluate the internal energy and the mass of gas, some analytical expressions of the variation of internal energy and mass must be derived in function of time, or in function of the crank angle since rotation speed is known. Those expressions can be derived from the conservations of energy and of mass. The differential equations, solved at each crank angle step, are presented hereunder.

$$\frac{dU}{d\theta} = \frac{\dot{Q}}{\omega} - \frac{PdV}{d\theta} + \frac{1}{\omega} \sum (\dot{M}_{in}h_{in} - \dot{M}_{out}h_{out})$$

$$\frac{dM}{d\theta} = \frac{1}{\omega} \sum (\dot{M}_{in} - \dot{M}_{out})$$

Those derivatives are function of the variables at the previous crank angle step and can be used in an Euler-Forward solver.

Euler Forward solver has firstly been chosen for its simplicity of implementation. However it is known that it does not show the largest accuracy. The latter is actually of order of the squared value of the crank angle step. Moreover Euler Forward is not an adequate solver for stiff problems such as the small volume encountered in a scroll expander in the discharge chamber. The choice of the solver is very important and should result from a compromise between the precision and the computational time required.

A literature review has been conducted about the different explicit solvers that can be used in stiff problems. Fourth order Runge Kutta (RK4) is the second most famous solver. Its precision is of the order of the crank angle step exponent 4. The inconvenient of that solver is that it creates intermediate points between the points  $n$  and  $n + 1$ . To overcome this issue that leads to an increase of the computational time, a fourth and fifth order Runge-Kutta-Fehlberg – or simply RKF 45 - solver could be used. It uses the RK developments of fourth and fifth order and allows modifying the crank angle step to decrease the computational time. All those solvers are one step solver which are functions of the previous crank angle step only. The last solver is a multistep solver named Adams-Bashforth-Moulton solver – or ABM. This solver is based on a predictor-corrector scheme. The predictor is an explicit step that will define a new fictitious point. That point is used by an implicit step, called the corrector, and defines the point  $n + 1$ . The main advantage is that this solver only creates one intermediate point because it is function of the previous values already known. However the first steps need to be solved by a different solver since it requires several previous steps.

Those solvers have been compared on a simple stiff problem given by

$$\frac{dY}{dt} = -aY(t)$$

where  $a$  is a positive constant. The solution of this differential equation is rather simple and is equal to the exponential of the product of  $-a$  times  $t$ . The error between the solver solution and the analytical solution is presented in Figure 2. RK4 and ABM solvers are pretty close in terms of precision and in computational time. The precision of RKF45 is very good and can be modified by specifying the crank angle step limits which define the modification of the crank angle step size. From that simple example, it can clearly be seen that Euler Forward is not the ideal solution but provides a good compromise between precision and computational time. In order to improve the simulation accuracy, RKF45 or ABM solver should be implemented.

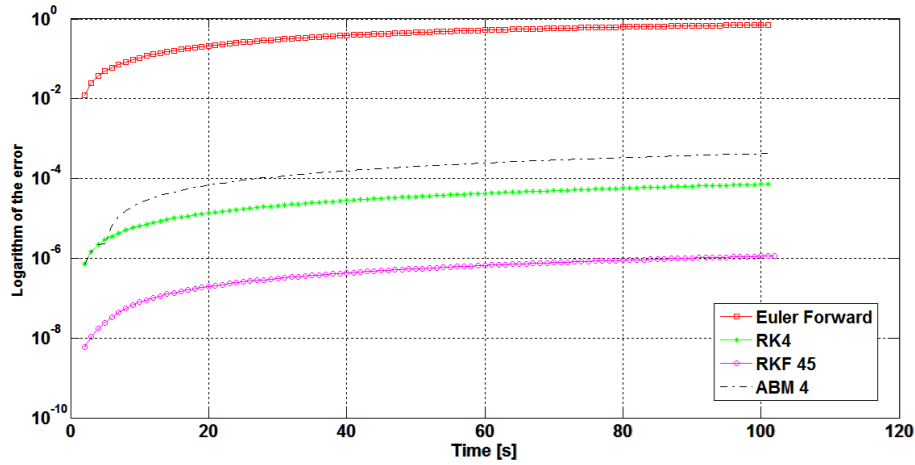


Figure 2 : Logarithm of the difference between the exact solution and the solver solution for four solvers

### 2.2.3 Mass flow modeling

The second part consists in the evaluation of the different mass flow rates. This includes the supply, the exhaust and the leakage mass flows. The modeling of the mass flows in a scroll compressor is a subject widely treated in literature, from simple 0D models to highly complex 2D model [5, 8]. In order to choose correctly how to model those flows, a literature review has been conducted. Firstly, some rather simple 0D models have been chosen. This is mostly to avoid too much calculation time of the algorithm but Yong et al. confirm our choice. Indeed, they developed in [8] a 2D model and conclude that a simple 0D model can be accurate enough depending on whether the ratio of the height of the leakage gap over the length of the leakage path is small or not. If it is small, a 0D model is enough, otherwise the complexity should be increased.

The following equations define the most common mass flow model, which is the isentropic flow model. It has been studied by several authors and compared with experimental results [9]. The biggest disadvantages of this model is that it does not take into account friction. So, if the flow path is narrow and long, friction will have a major importance. However, its efficiency for leakage with a short flow path has been demonstrated with experimental results.

$$\dot{M} = \begin{cases} A\sqrt{2P_h\rho_h} \sqrt{\left(\frac{\gamma}{\gamma-1}\right) \left(\left(\frac{P_l}{P_h}\right)^{\frac{2}{\gamma}} - \left(\frac{P_l}{P_h}\right)^{\frac{\gamma+1}{\gamma}}\right)} & \text{if } \frac{P_l}{P_h} > \left(1 + \frac{\gamma-1}{2}\right)^{\frac{\gamma}{\gamma-1}} \\ A\sqrt{2P_h\rho_h} \frac{\gamma}{\gamma+1} \left(\frac{2}{\gamma+1}\right)^{\frac{1}{\gamma-1}} & \text{otherwise} \end{cases}$$

To overcome the friction issue of the isentropic flow model, different models have been proposed. Bell fixes the problem by introducing a correction coefficient on the mass flow [10] but it has to be calibrated with experiments. Ishii et al. also proposed a solution [9] where they did some tests and compared different models of flow and come to the conclusion that a model of incompressible, viscous and fully turbulent is accurate enough. In such a model, the mass flow rate is computed by

$$\dot{M} = A \sqrt{\frac{2D_h\rho_h\Delta P}{fL}}$$

So, for the model of the supply and the exhaust mass flows, we choose to represent them by an isentropic flow. Indeed, the path flow is rather short and should not be submitted to friction too much.

For the internal leakages, literature distinguishes two types of leakages. The first one is the one called flank leakage and is happening between two consecutive chambers along the spirals. This one can also be modelled as an isentropic flow for the same reasons as above.

Finally, the radial leakages are the second type of leakage inside a scroll machine. It goes from one chamber to the next one radially and over the spiral. This leakage is more likely to have friction involved because the leakage path is quite long comparing to its height. So, we choose a frictional model as [6, 9] mentioned it.

#### 2.2.4 Heat transfers

Heat transfers appear between the fluid and the scroll at the inlet and the exhaust of the machine, between the fluid and the scroll wraps and between the scroll wraps and the ambience.

The heat transfer coefficients are modeled by the Dittus-Boelter relation with some corrections. The heat transfer coefficient equation for the Dittus-Boelter relation is given hereafter.

$$h_{DB} = 0.023 \frac{\lambda}{D_h} Re^{0.8} Pr^{0.4}$$

The heat transfer coefficient is then corrected by multiplying the Dittus-Boelter coefficient by two correction factors. The first one -  $K_1$  - has been investigated for the spiral heat exchanger [11] and it is used to take into account the spiral geometry. The moving involute introduce a forced convection heat transfer and it is the purpose of the second coefficient -  $K_2$  - to include that phenomenon [12]. The relations for the coefficients are given by

$$K_1 = 1 + 1.77 \frac{D_h}{r_c}$$

$$K_2 = 1 + 8.48(1 - \exp(-5.35 St))$$

The heat transfers are computed at each crank angle step between each chamber and its walls and between the ambience and the scroll expander.

#### 2.2.4 Forces evaluation

The axial force is easy to compute and is given by the following equation

$$F_{ax} = P \frac{V}{H}$$

The radial force is decomposed into its x and y components. The problem resumes to find the normal direction to the involute because the area on which the force is applied can be numerically computed knowing the conjugacy angles of the chamber. The components of the radial force are then given by

$$F_x = PA \frac{n_x}{\sqrt{n_x^2 + n_y^2}}$$

$$F_y = PA \frac{n_y}{\sqrt{n_x^2 + n_y^2}}$$

Where the normal components are defined by

$$n_x = -r_b(\theta - \varphi_0) \sin(\theta)$$

$$n_y = r_b(\theta - \varphi_0) \cos(\theta)$$

Finally, the radial force can be obtained by

$$F_{rad} = \sqrt{F_x^2 + F_y^2}$$

### 2.2.5 Mechanical losses

The most important source of mechanical losses in a scroll compressor is often the friction between the moving involute and the thrust bearing [13]. In order to compute this loss, a simple force balance on the moving involute can provide the effective force acting on that involute. The effective force is the difference between the axial force resulting from pressure inside the chamber and the counter force that is applied in order to maintain the two spirals together. With the proper friction coefficient and a dry friction model, the effective force can be transformed into a friction force and a friction torque with the radius where the force applies. Finally, including the rotation speed, the friction power loss is obtained.

### 3. Numerical simulations

Simulation results are presented hereunder in graphs with normalized axes. These are the first results and in order to be trustworthy the model still need to be calibrated. However those results can provide trends in design. In the following paragraphs, every geometric characteristic, such as leak gaps, geometric angles... is kept constant. Otherwise it is specified. The simulations are run with water as working fluid.

Figure 3 presents a P-V diagram for two different supply pressures. As we can see the model can take into account under- and over-expansion. The pressure loss at the supply port of the expander is also modeled and visible in the P-V diagram. The pressure loss at the admission is however better illustrated in the Figure 4. In that Figure, the pressure during a full revolution is plotted with respect to the crank angle. The different curves correspond to cases where the radius of the admission port or the rotation speed vary. Figure 4 illustrates the pressure loss that occurs in the suction chamber.

The ideal case would be to have a constant pressure along the revolution but two phenomenon reduce the efficiency, especially at high speed. The first one is that the flow can be choked and this should not happen normally since the pressure ratio is very low but it is more likely to happen at high speeds. The major issue comes from the fact that the moving spiral can pass over the admission port. Tip geometry can be modified to avoid that, however, this is not implemented in the algorithm. From Figure 4, it is clearly obvious that operating at high speed could lead to significant pressure drop and thus, to efficiency and produced power reductions. This leads to a major conclusion: since the clearance volume is not a source of loss in scroll expander, the tip geometry should be designed in such a way that the suction port has the most important area.

The isentropic efficiency is defined by the following equation and is presented in the Figure 5 with respect to pressure ratio and rotation speed.

$$\epsilon_s = \frac{\dot{W} - \dot{W}_{loss}}{\dot{W}_s}$$

From this graph, we can clearly see that the model is able to represent correctly the efficiency curve of the scroll machines. It is also known that the speed has a positive impact on leakage and since the frictional losses are low in this case the efficiency tends to increase if the speed is increased. It is also important to note that the gain obtained is a degressive function of the rotational speed. Working with a scroll expander using high rotational speed seems to be a good solution if friction can be maintained low. Moreover, leakage is a difficult

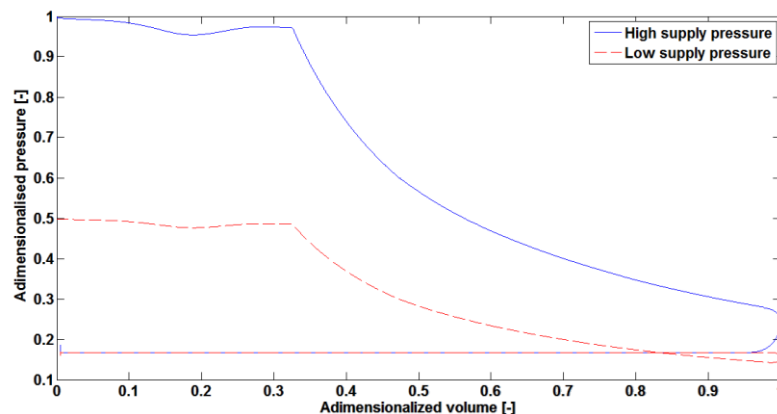


Figure 3 : Pressure-volume diagram for different rotational speeds. Both axes have been adimensionalized by dividing the variable by a constant

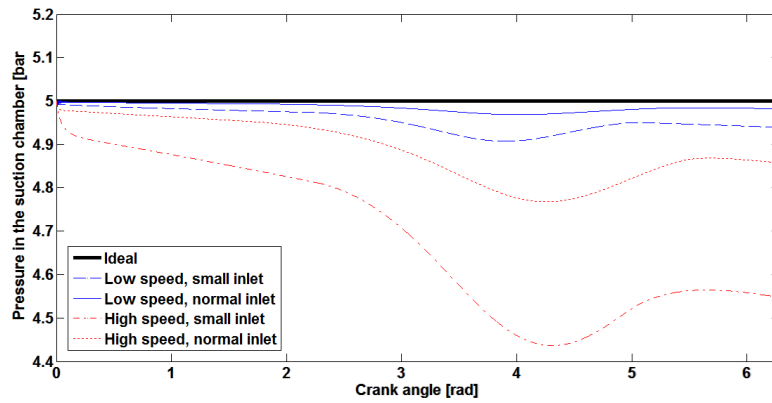


Figure 4 : Pressure in the suction chamber in function of the crank angle. Results are presented with different cases where rotational speed and inlet radius vary.

parameter to control while the control of friction is easier. Indeed, the choice of adequate materials or coatings and the anti-rotation mechanism could greatly help reducing friction. On the other side, internal leakage, particularly flank leakage, can only be reduced by introducing a high viscosity fluid. The choice of that fluid is particularly difficult since the operating environment is very harsh (high temperature, high pressure ...). In Figure 5, the maximum of the efficiency curve usually corresponds to the built-in volume ratio, which can be related to a pressure ratio regarding the operating conditions. However we can see in that Figure that the maximum is drifting with an increase of rotational speed. This is due to the fact that the leakage increase a little bit the pressure at the end of the expansion. Increasing the speed reduces the leakage and show a maximum closer to the built-in volume ratio.

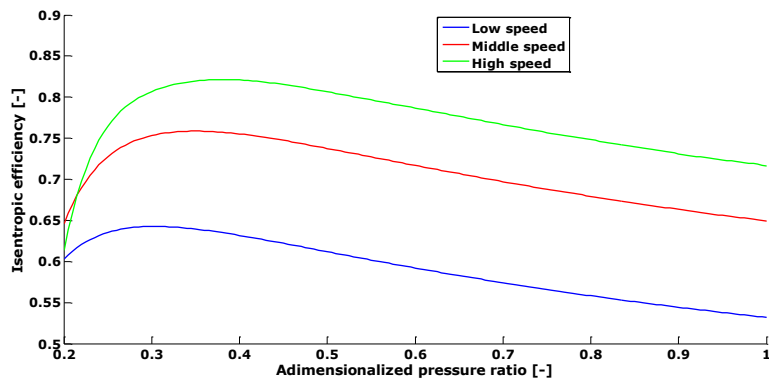


Figure 5 : Isentropic efficiency in function of a normalized pressure ratio for different rotational speeds. The pressure ratio has been normalized regarding to the pressure ratio corresponding to the built-in volume ratio

Figure 6 illustrates the different losses taken into account by the model and their impact on the scroll performance. For this graph, we have taken parameter close from what we could expect in an actual scroll compressor. The flank leakages represent the biggest source of losses and the other are much smaller. Every loss seems also not to vary significantly with the pressure ratio, except the loss due to fixed volume ratio of the expander, which are called "Inadapted  $\tau_v$  loss". That loss induces over- or under- expansion.

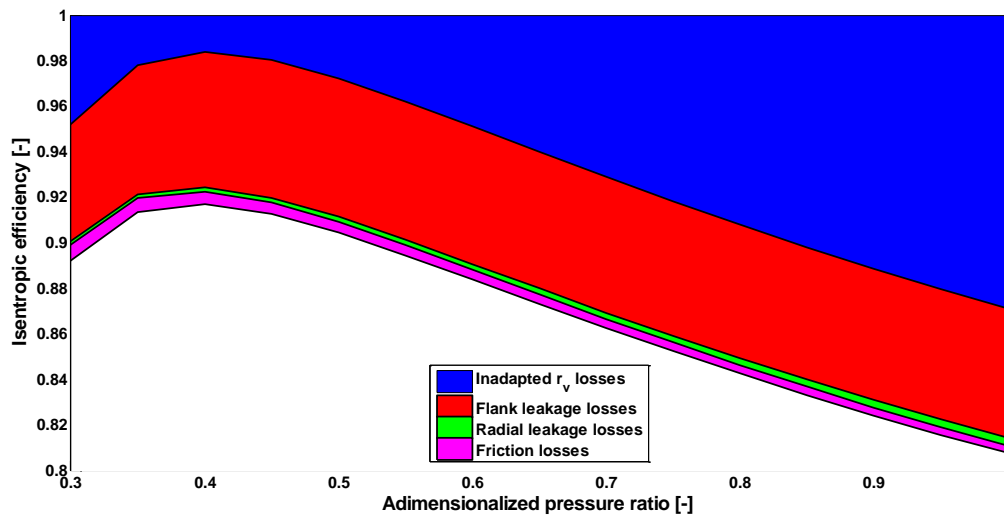


Figure 6 : Losses in a scroll expander plotted in an efficiency graph

#### 4. CONCLUSION

A model of scroll expander has been developed and we are able to see the influence of various parameters such as the geometry, the leakage gaps or the working conditions. This model will be used to design a scroll expander suited for waste heat recovery in a light vehicle. Some important conclusions can already be drawn. Indeed, the design of the inlet port should be carried out correctly since a low molar mass fluid will require higher rotational speeds.

The scroll expander model could also benefit from a few improvements. The calculation time needs to be optimized and some numerical solvers with adaptive crank angle step could be a solution. Other types of solvers can also be implemented. Last improvement should be the calibration of the model on some experiments.

In conclusion, several improvements can still be made but the model is ready and properly working. It provides results that are for now more qualitative but still useful to provide guidelines for the design of an expander.

#### 5. BIBLIOGRAPHY

- [1] W. J. Still, "Internal combustion engine". England Patent 1230617, 19 June 1917.
- [2] PSA Peugeot Citroën, "Thermal recuperation : Rankine Cycle," in *Highly Integrated Combustion Electric Propulsion System : Final event*, Florence, 2011.
- [3] PSA Peugeot Citroën, "Internal Work," 2011.
- [4] Y. Chen, *Mathematical modeling of scroll compressors*, 2000.
- [5] I. Bell, *Theoretical and experimental analysis of liquid flooded compression in scroll compressors*, 2011.
- [6] V. LEMORT, *Contribution to the Characterization of Scroll Machines in Compressor and Expander*

Modes, 2008.

- [7] B. R. SCHAFFER and E. A. GROLL, "Parametric representation of scroll geometry with variable wall thickness," in *International Compressor Engineering Conference*, Purdue, 2012.
- [8] H. YONG, "Leakage calculation through clearances," in *International Compressor Engineering Conference*, Purdue, 1994.
- [9] N. Ishii, K. Bird, K. Sano, M. Oono, S. Iwamura and T. Otokura, "Refrigerant leakage flow evaluation for scroll compressor," in *International Compressor Engineering Conference*, Purdue, 1996.
- [10] I. H. Bell, E. A. Groll, J. E. Braun and T. Horton, "A computationally efficient hybrid leakage model for modeling leakage in positive displacement compressors," in *International Compressor Engineering Conference*, Purdue, 2012.
- [11] N. Tagri and R. Jayaraman, "Heat transfer studies on a spiral plate heat exchanger," *Trans. Inst. Chem. Eng.*, pp. 161-168, 1962.
- [12] K. Jang and S. Jeong, "Experimental investigation on convective heat transfer mechanism in a scroll compressor," *International Journal of Refrigeration*, pp. 744-753, 2006.
- [13] S. HAJIME, I. TAKAHIDE and K. HIROYUKI, "Frictional characteristics of thrust bearing in scroll compressor," in *International Compressor Engineering Conference*, Purdue, 2004.